Barrier properties of small gas molecules in amorphous cis-1,4-polybutadiene estimated by simulation

Patricia Gestoso, Marc Meunier

Molecular Simulation
Journal of
Experimental Nanoscience

Taylor & Francis
Taylor & Francis Group

Barrier properties of small gas molecules in amorphous cis-1,4-polybutadiene estimated by simulation

Journal:	*Molecular Simulation/Journal of Experimental Nanoscience*
Manuscript ID:	GMOS-2008-0086.R1
Journal:	Molecular Simulation
Date Submitted by the Author:	02-May-2008
Complete List of Authors:	Gestoso, Patricia Meunier, Marc; Accelrys Ltd
Keywords:	Solubility, Diffusion, Selectivity, TST, Polybutadiene

Barrier properties of small gas molecules in amorphous cis-1,4-polybutadiene estimated by simulation

Abstract

The solubility and diffusivity of small gas molecules in amorphous cis-1,4-polybutadiene (cis-PBD) were estimated in the temperature range 250-400 K using both molecular dynamics simulations and the Transition State Theory implementation of the Widom insertion method. A comparison of the methods is given and the results obtained are compared with available experimental data. The accuracy in predicting diffusion and solubility coefficients of a range of small gas molecules in an amorphous polymer of both methods is good when compared to experimental values. The effects of the temperature and the models size are also examined. Selectivity to oxygen and nitrogen are estimated for the various models studied as well. This work shows the potential of computational methods for the prediction of physical properties of industrial importance like selectivity.

Keywords: *Solubility, Diffusion, TST, Selectivity, Simulation, Polybutadiene*

Barrier properties of small gas molecules in amorphous cis-1,4-polybutadiene estimated by simulation

P. GESTOSO* , M. MEUNIER

Accelrys, 334 Science Park, Cambridge, CB4 0WN United Kingdom

Abstract

The solubility and diffusivity of small gas molecules in amorphous cis-1,4-polybutadiene (cis-PBD) were estimated in the temperature range 250-400 K using both molecular dynamics simulations and the Transition State Theory implementation of the Widom insertion method. A comparison of the methods is given and the results obtained are compared with available experimental data. The accuracy in predicting diffusion and solubility coefficients of a range of small gas molecules in an amorphous polymer of both methods is good when compared to experimental values. The effects of the temperature and the models size are also examined. Selectivity to oxygen and nitrogen are estimated for the various models studied as well. This work shows the potential of computational methods for the prediction of physical properties of industrial importance like selectivity.

Keywords: *Solubility, Diffusion, TST, Selectivity, Simulation, Polybutadiene*

* contact author: patriciag@accelrys.com

Accelrys, 334 Science Park, Cambridge, CB4 0WN United Kingdom

1. Introduction

Many industrial applications take advantage of the diverse barrier properties of polymers. Amongst them, gas separation for high purity gases production, food packaging and the beverage industry are most common.[1] More advanced applications are concerned with the development of new polymer membranes for higher selectivity ratio.

Modelling of gas sorption in polymers is a very difficult and presents a permanent challenge to theoreticians and experimenters.[2] The gas permeation process is defined as a "solution diffusion" process, where at first the gas permeant is dissolved on the surface and then the gas molecules slowly diffuse through the polymer membrane.[3] Predicting the permeability directly from simulation is known to be quite difficult. The advantage of such permeation model is that it allows considering each process (solubility and diffusion) separately and then combining the results to calculate the permeability

$$P = D \times S \qquad \text{Eq. 1}$$

where D is the diffusion coefficient and S is the solubility of penetrants.[4]

At sufficiently low pressure the solubility is obtained from:

$$C = S \times p \qquad \text{Eq. 2}$$

where C is the solubility, p is the pressure and S is the solubility coefficient.

The prediction of physical and chemical properties by computational methods is becoming more and more common in the research area thanks for part to the available computational power at a low cost. Various computational methods exist to model amorphous materials (e.g. polymers) that are readily available to the modeller: molecular dynamics (MD), Monte Carlo, Transition State Theory (TST), mesoscale simulations to name but a few. For a complete review of methods see [ref. 5-6]. Recently, molecular dynamics simulations of up to 3 ns were performed to estimate the diffusivity of small gas molecules in amorphous cis-1,4-polybutadiene (Cis-PBD). [7]

Polymers are undoubtedly widely used for "permeation materials" (e.g. in packaging, membrane for gas separation, etc) thanks to their chemical resistance. Currently, efforts in research and development concentrate on understanding the phenomena involved during gas transport through membranes as well as to synthesize novel polymers with better separation properties. The permeability of a specific gas molecule (e.g. O_2) in different polymers varies only slightly. It has been shown that simple relationship can be found between the ratios of the permeability constants for a series of gases through different polymers.[8-9] In fact, it has been shown too that similar relationship can be found for the diffusion and the solubility.

Main factors affecting small penetrants permeability in polymeric material are: the free volume and its distribution,[10-11] the density,[12] the temperature and pressure, the crystallinity,[13] the polymer chain length,[12] mobility[14] and packing,[10] the solute size[15] and affinity for the material. In addition, computational parameters used in the simulations such as the type of force field employed and the size of the model also affect the permeability value computed.[7] Increase of temperature generally leads to a decrease of the solubility and conversely for the diffusion. For all three physical quantities P, S and D, the temperature dependence can be described by a Van't Hoff-Arrhenius equation.[16] In particular for the solubility:

$$S(T) = S_0 \exp(-\Delta H_S / RT) \qquad \text{Eq. 3}$$

where ΔH_S is the molar heat of sorption.

In this context, this work is oriented towards the assessment of atomistic simulation techniques for the calculation of the barrier properties of cis-1,4-polybutadiene (cis-PBD) melts. First, two different methods, molecular dynamics (MD) and Transition State Theory (TST) will be compared in terms of solubility and diffusion coefficients as well as their capabilities to reproduce their dependence with temperature. Additionally, the effect of chain length on the predictions will be also evaluated. Finally, the ability of both simulation methods to predict selectivity will be compared.

2. Methodology

Computational details of the simulation runs are given in this section as well as a description of the atomistic models used.

2.1. Models

2.1.1. Short chains models

Polymer models were created using the Amorphous Cell module of the Materials Studio suite of software[17] based on the "self-avoiding" random-walk method of Theodorou and Suter[18] and on the Meirovitch scanning method.[19] Amorphous Cis-PBD 3D models consisted of 10 chains of 30-monomers oligomers and were equilibrated using a temperature cycle protocol under periodic boundary conditions (Figure 1).[20] For a full description of the methodology employed to build the equilibrated polymer models at the various temperature of study please see ref. [7].

Polymer models validation was ensured by checking the convergence of the total energy at the end of the molecular dynamics runs as well as a density value and cohesive energy density close to that of experiment.[7] Moreover, plotting the total, intra and inter carbon-carbon pair correlation functions (Figure 2) shows that the intra molecular pair correlation function g^{CC}_{intra} (r) has a limit value of zero and the inter molecular pair correlation function g^{CC}_{inter} (r) has a limit value of one at long range, thus demonstrating well equilibrated configurations.

2.1.2. Long chains models

Polymer models consisting of one single chain of 300 monomers were created using a Monte Carlo based method similar to the short-chains models described above. This was done in order to study the effect on

diffusion and solubility of the presence in these short chains models of too many chain ends (as compared to the real material), and therefore of added free volume. It has been suggested that this is one of the main factors of discrepancy between simulated and experimental values.[7] The models were validated using similar procedure that that described in section 2.1.1.

2.1.3. Sorbates

The geometry of the sorbate molecules were optimised using the DFT code DMol[3] [17,21-22] using default settings. Sorbates were inserted at the same time that the polymer chain using the Amorphous Cell module.[17]

2.2. Computational Methods

2.2.1. Transition State Theory

The Transition State Theory (TST) method was introduced by Arrizi, Gusev and Suter for polymers.[23-26] The method, as implemented in the *InsightII gsnet* and *gdiff* subroutines[27] is initiated as a 3-D fine resolution grid laid on the relaxed polymer configuration. Then, a spherical probe of radius equal to that of the gas penetrant is inserted in all grid points and the resulting non-bonded energy, $E_{ins}(x, y, z)$, is calculated between the test probe and all atoms of the polymer matrix. Following the Widom method[28-29] the excess chemical potential, μ_{ex}, is calculated using:

$$\mu_{ex} = RT \ln \left\langle \exp\left(-\frac{E_{ins}}{k_B T} \right) \right\rangle \qquad \text{Eq. 4}$$

where R is the universal gas constant, T is the temperature, k_B the Boltzmann constant and the brackets, < >, denote averages over all grid points and probe insertions. Finally, the solubility coefficient is calculated from the excess chemical potential, μ_{ex}, through:

$$S = \exp\left(-\frac{\mu_{ex}}{RT} \right) \qquad \text{Eq. 5}$$

The identified sorption sites are separated by high-energy barrier surfaces; therefore, penetrant diffusion can be seen as a series of infrequent transitions between adjacent microstates. In TST, in order to calculate the diffusion coefficient the sorbates are displaced in the coarse-grained lattice over a large number of time steps and a large population of ghost walkers through a kinetic MC (kMC) scheme.[30-31] The diffusion coefficient is then calculated from the value of the mean square displacement (MSD) from the trajectories of all penetrant walkers:

$$D = \lim_{t\to\infty}\left\{\frac{\left\langle\left[\mathbf{r}_p(t)-\mathbf{r}_p(0)\right]^2\right\rangle}{6t}\right\} \qquad \text{Eq. 6}$$

where the brackets, < >, indicate average over all trajectories and all time origins. Finally, the permeability is calculated through eq. (1).

The thermal fluctuations of the polymer matrix are taking into account through the smearing factor "Δ^2", which is related to the mean square displacement of the matrix segments from their equilibrium positions.

The TST method has the advantage of extending the time-scale of the observation when compared to classical dynamics; however, it involves a number of assumptions. First, the polymer matrix response to the guest molecule should be elastic. This is due to the rather simplistic form of calculating the smearing factor, which limits the application of the method to the behavior of small molecules which presence does not affect the polymer environment. Second, the shape of the penetrant is supposed to be isotropic. As the penetrant size increases and its shape becomes anisotropic, conventional TST fails to capture the corresponding transport behavior.

In this work, the grid size used was set to 0.3 Å, in agreement with typical values found in the literature for TST calculations.[3,32-35] The smearing factor, Δ^2, was calculated for each penetrant through a self-consistent scheme involving information about the mean square displacement of all the polymer atoms from their respective equilibrium positions. The mean square displacement was calculated from a 50ps NVT MD

simulation. The self-consistent scheme converged when the relative difference between two successive Δ^2 values was within 2.5%. The total duration of the kMC procedure was 10^{-4} s and the MSD was averaged over the trajectories of 1000 penetrant walkers.

All penetrant molecules were represented as single, spherical, united-atom sites whose short-range interactions with the polymer atoms are described through a 9-6 Lennard-Jones (L-J) potential, the values of collision diameters, σ, and the well depths, ε, already reported in the literature for the COMPASS forcefield.[17,36] The non-bonded interactions were truncated at 9.5 Å. All polymer atoms were represented explicitly and the potential function and atomic parameters can be found elsewhere.[36] The reported values correspond to the sampling over five structures and the error bars to standard deviations of the distributions of the calculated values.

2.2.2. Molecular Dynamics

Molecular dynamics simulations were employed to estimate the diffusion coefficients of the sorbates in both short and long chains models. Four geometry optimised sorbates were randomly inserted in the model cells and long NVT simulations were performed. The complete methodology has been described elsewhere and is not detailed here.[7]

3. Results and Discussion

In this part we report the results of the computation of the solubility values using both Metropolis Monte-Carlo and TST methods. Comparison between the two methods is given as well as comparison with experimental data when available.

3.1. General

We report first the variation of the total and free volume of the models. For the short chains models, the total and free volume are varying linearly with the temperature in the temperature range 250 – 400 K, as shown on graphs 3 and 4. The free volume represents 38.6 % of the total volume at 250 K, 40.2 % at 300 K, and 43.7 % at 400 K. For the long chain models the total free volume represents 39.2 % at 300K, thus slightly less than the short chains models as expected due to a reduction in the number of chain ends at equal density.

3.2. Solubility coefficients

The comparison between solubility coefficient results obtained from TST calculations at T=300K for short and long chain models and experimental results are shown in Table 1. As can be seen, the simulation results follow the experimental tendency, i.e., the solubility parameter increases with the size of the molecule. This behaviour has been well documented in the literature. Additionally, it can be seen that there is a very good quantitative agreement between experiments and TST, especially for long chains, with the exception of CO_2. The failure to capture the CO_2 transport behaviour is inherent to the restrictions of the current implementation of TST where all molecules are considered spherical. As CO_2 has an anisotropic shape, conventional TST fails to capture the corresponding transport behaviour.[37]

Figure 5 shows the dependence of the solubility coefficient on temperature in the range 250K ≤ T ≤ 400K. As expected, solubility decreases with temperature, i.e., as the temperature increases, the gas molecules experiment more difficulty to condense. This behaviour is in agreement to the experiments (CO_2 in PET[39]) and simulations (CO_2 and He in PE4,[40] CO_2 and CH_4 in polyetherimide,[41] CH_4 and CO_2 in HDPE[42], n-alkanes in poly(dimethylsilamethylene)[43] and O_2, N_2 and CH_4 in PE for long and short chains[37]).

From Figure 5 is it also possible to calculate the heat of solution. The values obtained were 27.69 kJ/mol for CO_2, 19.83 kJ/mol for CH_4, 18.53 kJ/mol for Ar, 15.32 kJ/mol for O_2, and 14.54 kJ/mol for N_2. For all penetrants it was found that the dependence with temperature followed an Arrhenius behaviour (eq. 3). The fact that the heat of solution values are in general more positive as the solubility of the permeant increases is in contradiction with experimental evidence,[38,44] pointing out the limitations of TST to capture the dependence of solubility with temperature.

3.3. Diffusion Coefficients

Table 2 presents the comparison between the diffusion coefficients from Molecular Dynamics calculations, TST and experimental results at 300 K for short and long chains models. As can be seen, the predicted values from simulations and TST are in good agreement with experimental data, with low values of the RMSD. Deviations are of the same order as in experimental reported data. The experimental reported values of the penetrants in [13] come from two different publications: [45] and [46] thus making comparison difficult. Though, the ranking of the penetrants between experiments should be similar, errors while combining data might alter this (as it is the case here for O_2). Overall, theoretical values are systematically overestimating the experimental data; behaviour that has been already observed and reported in the literature.[7] Long chain models perform better than short chains ones, as expected from Figure 3 showing the comparison of free volume in the models. This can be explained as experimental values were measured for very long chain

samples, which have smaller free volume and higher density when compared to short chains. Free volume and density play a fundamental role in diffusion, as has been demonstrated elsewhere;[37] therefore, it is to expect that the diffusion coefficient values obtained for the long chain models are closer to experimental values than those from short chain models. Therefore, although the making of such long chains models are computationally more expensive than the short chains ones, it results in an improvement of the predictability of the methods.

The dependence of diffusion coefficients with the inverse of temperature is plotted in Figure 6 using TST. As can be seen, the diffusivity increases with the temperature, behaviour in perfect agreement with experimental and simulation results in the literature. The diffusion activation energies were calculated as

$$D = D_0 \exp(-E_D / RT) \qquad \text{Eq. 7}$$

The values obtained for E_D are 29.70 kJ/mol for CH_4, 29.21 kJ/mol for Ar, 22.11 kJ/mol for O_2, and 26.18 kJ/mol for N_2, which compare well with experimental activation energies in the range of 20-30 kJ/mol.[38,44] This is an improvement compared with the results obtained using MD techniques,[7] in which the values for the same penetrants were lower than 10 kJ/mol. For CO_2 the activation energy decreases with temperature as already reported for methane in polybutadiene.[7,10]

3.4. Selectivity

A key property for the design of novel material for gas separation is its selectivity. In this paper we investigate modelling methods to predict the selectivity of small gas molecules in cis-PBD. The selectivity is defined as the ratio of the permeability of two penetrants, e.g.:

$$Selectivity(O_2, N_2) = \frac{P_{O_2}}{P_{N_2}} = \frac{D_{O_2} S_{O_2}}{D_{N_2} S_{N_2}} \qquad \text{Eq. 8}$$

where P_{O2} is the permeability of oxygen and P_{N2} is the permeability of nitrogen. For the calculations, the MD selectivities were computed from MD diffusion coefficients and TST solubility coefficients for the respective penetrants, whereas for the TST selectivities both the diffusion and the solubility coefficients where extracted from the TST simulations.

Tables 3 and 4 report the selectivity data from experiment and from simulations. In general, it can be seen that the theoretical models predict correctly the trends for oxygen and nitrogen selectivity. However, in all cases the simulation underestimates the selectivity values when compared to experimental. It is interesting to notice that this underestimation appears to be more noticeable for TST than for MD models.

4. Conclusion

The barrier properties of the Cis-PBD for different small gas penetrants have been estimated using molecular dynamics and transition state transition simulations techniques. A molecular model made of one single long chain was created to gain insights on known issues due to incorrect free volume distribution and size in molecular models made of many short chains. There is an overall good agreement between experiments and the results from both methods for solubility and diffusion coefficients; although, as expected, the values corresponding to the long chain models are in better agreement that those from the short chain models. This difference is more noticeable for MD simulations.

The heat of solution and the diffusion activation energy for the different penetrants in cis-PBD where derived from the TST plots of solubility and diffusion coefficient vs. temperature, respectively. The heat of solution for the different small molecules did not follow the trends reported in the literature. On the other side, the diffusion activation energies have a very good quantitative and qualitative agreement with experimental values, which was not the case in the MD simulations.[7]

Finally, the simulations are able to predict correctly the ranking of the selectivities for oxygen and nitrogen, although underestimating the values, the TST simulations to a higher degree than the MD simulations.

References

[1] J. Crank and G. S. Park. *Diffusion in Polymers*, Academic Press, London (1968).

[2] R. Patterson, Y. Yampol'skii, J. Phys. Chem. Ref. Data, **28**, 5, (1999).

[3] D. Hofmann, L. Fritz, J. Ulbrich, C. Schepers, M. Bohning, *Macromol. Theory Simul*., **9**, 293 (2000).

[4] Y. Tamai, H. Tanaka, K. Nakanishi, *Macromolecules,* **27**, 4498 (1994).

[5] A. R. Leach. Molecular Modelling, principles and applications. Pearson Education Limited, London (1996).

[6] J Leszczynski. COMPUTATIONAL CHEMISTRY: REVIEWS OF CURRENT TRENDS. *Jackson State University, USA* (1999).

[7] M. Meunier, *J. Chem. Phys.,* **123**, 134906 (2005).

[8] V. Stannett, Szwarc M., *J. Polymer Sci*., **16**, 89 (1955).

[9] H.L. Frisch, *Polymer Letters*, **1**, 581 (1963).

[10] R.H. Boyd, P.V.K. Pant, *Macromolecules*, **24**, 6325 (1991).

[11] H. Takeushi, R.J. Roe, J.E. Mark, *J. Chem. Phys*., **93**, 9042 (1993).

[12] H. Takeushi, *J. Chem. Phys*., **93**, 4490 (1990).

[13] S. Pauly in *Polymers Handbook*, 3rd Ed., J. Brandrup and E.H. Immergut Eds. Wiley, New York (1989).

[14] H. Takeushi, K. Okasaki, *J. Chem. Phys.*, **92**, 5643 (1990).

[15] S. Trohalaki, A. Kloczkowski, J.E. Mark, D. Rigby, R.J. Roe, *Computer Simulation of Polymers*, R.J. Roe Eds. Prentice-Hall: Englewood Cliffs, NJ, 220 (1991).

[16] D. W. Van Krevelen. Properties of polymers, 3rd edition, Elsevier (2003)

[17] Accelrys Inc. San Diego (2007).

[18] D.N. Theodorou, U.W. Suter, *Macromolecules*, **18**, 1467 (1985).

[19] H.J. Meirovitch, *J. Chem. Phys.*, **79**, 502 (1983).

[20] M.P. Allen, D.J. Tidelsey, *Computer simulation of liquids*. Oxford University Press, Oxford (1987).

[21] B. Delley, *J. Chem. Phys*., **92**, 508 (1990).

[22] B. Delley, *J. Chem. Phys.*, **113**, 7756 (2000).

[23] S. Arizzi. Diffusion of small molecules in polymeric glasses: a modelling approach. Ph.D Thesis, Massachusetts Institute of Technology, Boston, (1990).

[24] A.A. Gusev, S. Arizzi, U.W. Suter. D.J. Moll. *J. Chem. Phys*., **99**, 2221 (1993).

[25] A.A. Gusev, U.W. Suter. *J. Chem. Phys*., **99**, 2228 (1993).

[26] A.A. Gusev, F. Müller-Plathe, W.F. van Gunsteren, U.W. Suter. Adv. Polym. Sci., **116**, 207 (1994).

[27] Accelrys. InsightII. Accelrys Software Inc. San Diego (2007).

[28] B. Widom. *J. Chem. Phys*., **39**, 2808 (1963).

[29] B. Widom. *J. Phys. Chem.*, **86**, 869 (1982).

[30] R. June R, A.T. Bell, D.N. Theodorou. *J. Phys. Chem*., **95**, 8866 (1991).

[31] N.C. Karayiannis, V.G. Mavrantzas, D.N. Theodorou. *Chem. Eng. Sci*.,, **56**, 2789 (2001).

[32] D. Hofmann, J. Ulbrich, D. Fritsch, D. Paul. *Polymer*, **37**, 4773 (1996).

[33] D. Hofmann, L. Fritz, J. Ulbrich, D. Paul. *Polymer*, **38**, 6145 (1997).

[34] E. Kucukpinar, P. Doruker. *Polymer*, **44**, 3607 (2003).

[35] N.C. Karayiannis, V.G. Mavrantzas, D.N. Theodorou. *Macromolecules,* **37**, 2978 (2004).

[36] H. Sun. *J. Phys. Chem*. B, **102**, 7338 (1998).

[37] P. Gestoso, N. Ch. Karayiannis, *J. Polym. Phys. B*, in press (2008).

[38] G. J. van Amerongen, *J. Appl. Phys*., **17**, 972 (1946).

[39] Y.Mi, X. Lu, J. Zhou, *Macromolecules*, **36**, 6898 (2003).

[40] N.F.A. van der Vegt, *Macromolecules*, **33**, 3153 (2000).

[41] S.Y.Lim, T.T Tsotsis, M. Sahimi, *J. Chem. Phys.,* **119**, 496 (2003).

[42] N. von Solms, J.K. Nielsen, O. Hassager, A. Rubin, A.Y. Dandekar, S.I. Andersen, E.H. Stenby *J. Appl. Polym. Sci.*, **91**, 1476 (2004).

[43] V. E. Raptis, I.E. Economou, D.N. Theodorou, J. Petrou, J.H. Petropoulos, *Macromolecules*, **37**, 1102 (2004).

[44]. R. Cowling, G. S. Park, *J. Membrane Sci*., **5**, 199 (1979).

[45] S.A. Segazy, T. Segushi, S. Machi, *J. Appl. Sci*., **26**, 2937 (1981).

[46] E. Hegazy et al., *J. Appl. Polym. Sci*., **26**, 1361, (1981).

Tables

Table 1: Solubility coefficients ($x10^{-6}$ Pa^{-1}) for various sorbates at T= 300K; comparison of simulation methods and experimental data.

Penetrant	EXP 1 (a)	EXP 2 (b)	TST Short-chains	TST Long Chain
N_2	0.45	0.45	0.74	0.45
Ar	0.76	-	1.13	0.63
O_2	0.96	0.94	1.58	1.18
CH_4	-	-	2.69	1.33
CO_2	9.87	9.7	8.39	3.95
RMSD	-	-	0.418	1.481
RMSD (no CO_2)			0.259	0.085

(a) reference [13]

(b) reference [38]

Table 2: Diffusion coefficients for various sorbates (x 10^{-6}) at T= 300K; comparison of simulation methods and experimental data.

Penetrants	Exp (a)	MD Long Chain	TST Long Chain	MD Short Chains (b)	TST Short Chains
N_2	1.1 - 2.96	6.11	5.69	8.8	6.08
O_2	1.5	5.07	8.37	9.5	11.19
Ar	4.06	5.06	3.51	7.03	3.84
CH_4	2.25 (c)	2.96	3.22	7.5	3.47
CO_2	1.05	4.06	1.55	5.3	1.58
RMSD		2.58	3.35	5.52	4.59

(a) Reference [13]

(b) Reference [7]

(c) Reference [10]

Table 3. O_2 Selectivity at 300 K.

Penetrants	Exp. (a)	MD Long Chain	TST Long Chain	MD Short Chains (b)	TST Short Chains
N_2	0.67	0.46	0.26	0.43	0.25
Ar	2.15	0.53	0.22	0.53	0.25
CO_2	7.27	2.68	0.62	2.96	0.75

(a) Reference [13], average of both data for N_2

(b) Reference [7]

Table 4. N_2 Selectivity at 300 K.

Penetrants	Exp. (a)	MD Long Chain	TST Long Chain	MD Short Chains (b)	TST Short Chains
Ar	3.20	1.16	0.86	1.22	0.96
CO_2	10.81	5.83	2.39	6.83	2.95

(a) Reference [13], average of both data for N_2

(b) Reference [7]

Figure Captions

Figure 1: 3D model of amorphous cis-PBD at 300K with periodic boundary conditions.

Figure 2: Carbon-Carbon pair correlation function (thick line: inter-molecular rdf, thin line: intra-molecular rdf).

Figure 3: Circles: short chains models polymer total cell volume (average of five frames); Square: Long chain models (average over five frames).

Figure 4: Circles: short chains models polymer free volume (average of five frames); Square: Long chain models (average over five frames).

Figure 5: Logarithm of solubility coefficient (in cm^3(STP)/cm^3 Pa) as a function of reciprocal temperature for cis-PBD short-chains models. (diamonds: Ar; Cross: CH_4; Triangle: CO_2; Squares: N_2; Circles: O_2).

Figure 6: Logarithm of diffusivity coefficient (in cm^2/s) as a function of reciprocal temperature for cis-PBD short-chains models. (Diamonds: Ar; Cross: CH_4; Triangle: CO_2; Squares: N_2; Circles: O_2).

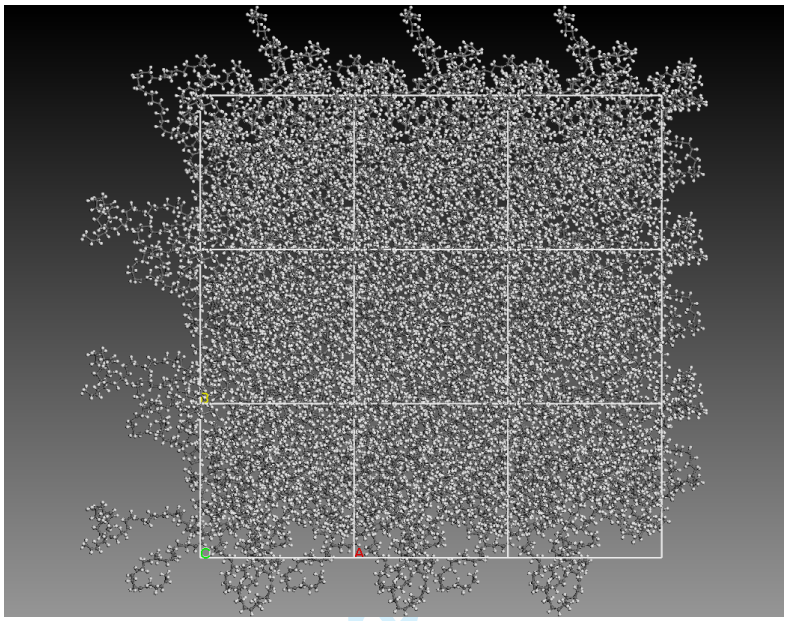

Figure 1. Gestoso and Meunier

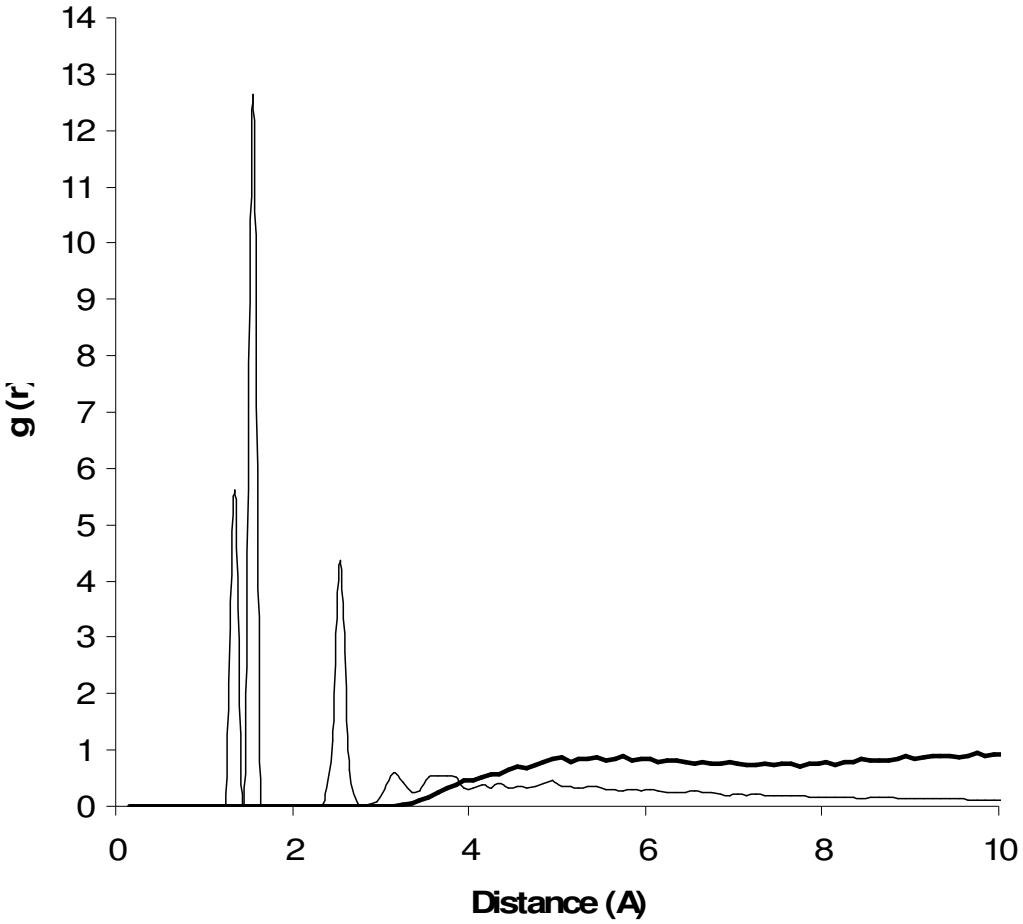

Figure 2. Gestoso and Meunier

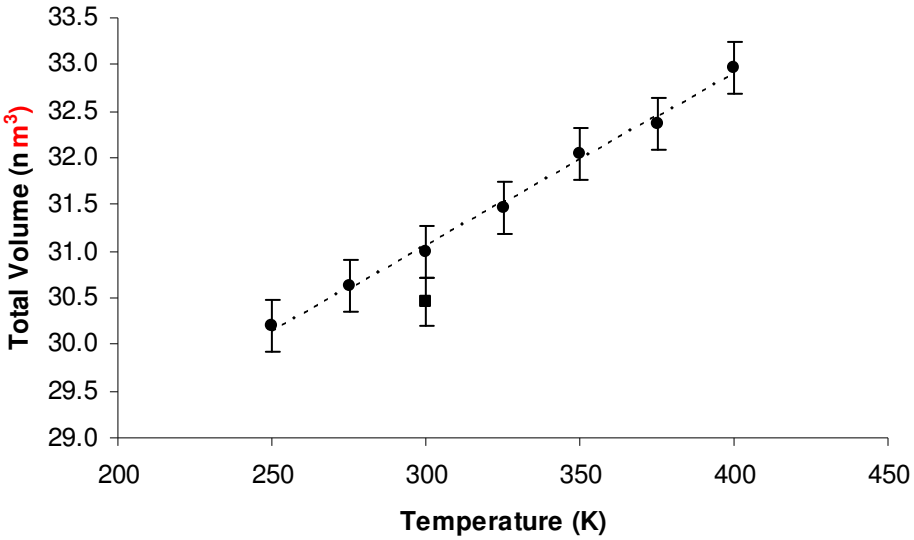

Figure 3. Gestoso and Meunier

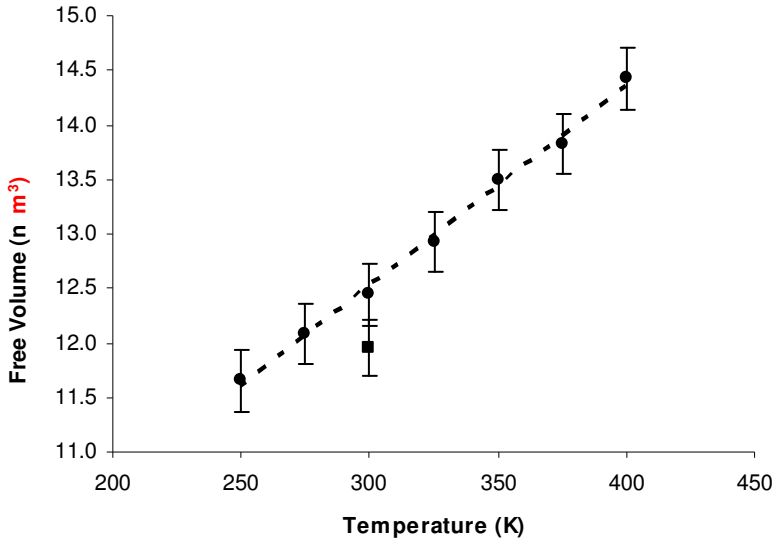

Figure 4. Gestoso and Meunier

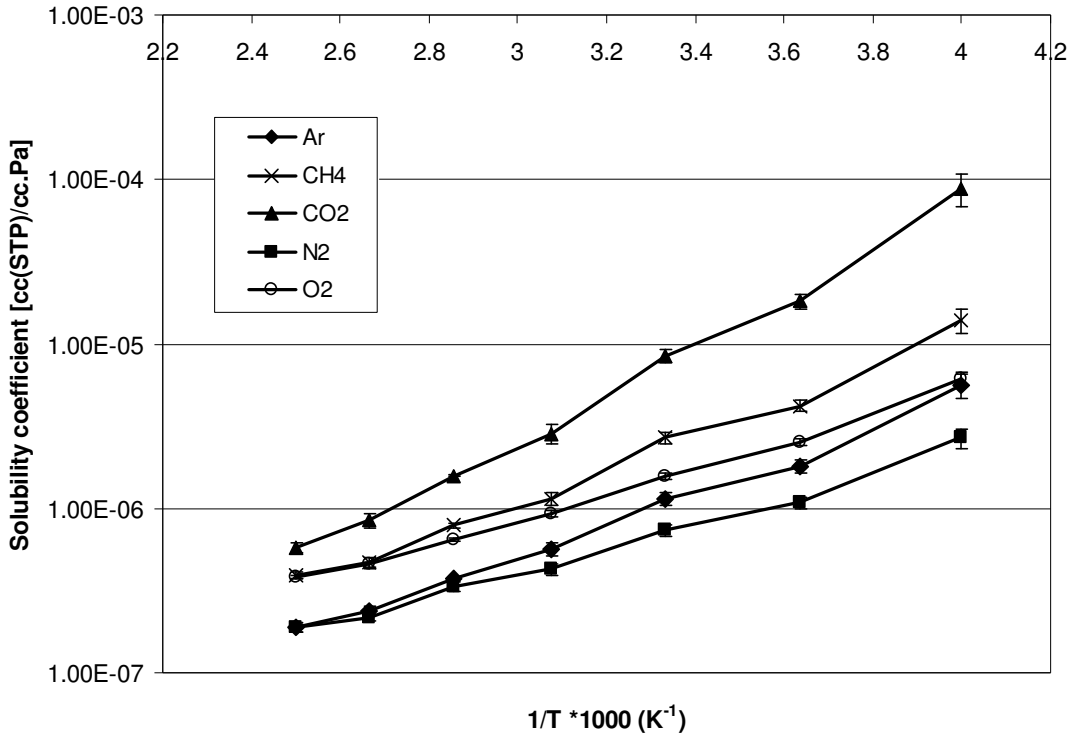

Figure 5. Gestoso and Meunier

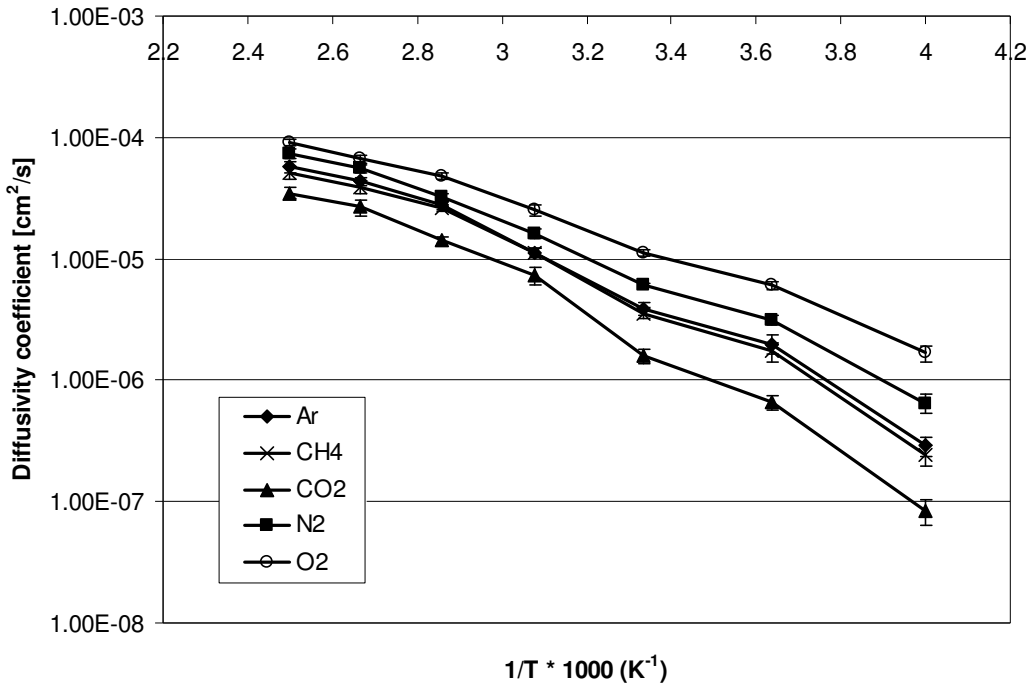

Figure 6. Gestoso and Meunier